IEEE Access
Multidisciplinary : Rapid Review : Open Access Journal

Received 1 August 2023, accepted 29 August 2023, date of publication 6 September 2023, date of current version 13 September 2023.
Digital Object Identifier 10.1109/ACCESS.2023.3312575

RESEARCH ARTICLE

Estimating Deficient Muscle Activity Using LSTM With Integrated Damping Neurons for EMG-Based Control of Robotic Prosthetic Fingers

DAIGO TOKUNAGA, (Student Member, IEEE), SATOSHI NISHIKAWA, (Member, IEEE), AND KAZUO KIGUCHI, (Senior Member, IEEE)
Department of Mechanical Engineering, Kyushu University, Fukuoka 819-0395, Japan
Corresponding author: Kazuo Kiguchi (kiguchi@ieee.org)

This work involved human subjects or animals in its research. Approval of all ethical and experimental procedures and protocols was granted by the Research Ethics committee of the Faculty of Engineering at Kyushu University under Application No. 2020-05.

ABSTRACT Robotic prosthetic hands can help perform the intended sophisticated movements of the upper limb, which can assist amputees to perform their daily activities. Although a robotic prosthetic hand can be controlled in real-time using the user's electromyography (EMG), which directly reflects the user's motion intention, some important EMG signals are usually lost owing to muscle deficiency. This study proposes a muscle activity estimator that is inspired by the muscle synergy across subjects to estimate the activity of the missing muscles in amputees in real-time. The proposed estimator learns muscle synergy from the EMG balance, finger joint angles, and the grasping force of healthy persons. The proposed estimator is developed as an artificial neural network (ANN) with a novel cell structure that combines long-short-term memory and damping neurons to analyze muscle dynamics. Furthermore, to improve the accuracy of learning muscle synergy, the muscles to be input to the estimator are selected by focusing on the enslavement of muscles and anatomical relationships. The effectiveness of the proposed estimator is evaluated by experiments. The results showed that the proposed estimator can contribute well to the realization of the intended sophisticated motions of the user.

INDEX TERMS Machine learning, muscle synergy, damping neuron, prosthetic robots, EMG estimation.

I. INTRODUCTION

Robotic hands, which mimic the movements of human hands, are used for various applications, such as extending physical functions or working in environments inaccessible to humans. Most anthropomorphic robotic hands are manipulated based on the operator's finger movements using data gloves, master robots, etc. [1], [2], [3], [4], [5], [6], and [7]. Some methods use inputs from the electromyography (EMG) of the operator's hand [8], [9], [10]. Therefore, robot hands are controlled in several ways to reflect the detailed movements of the operator's hand.

The associate editor coordinating the review of this manuscript and approving it for publication was Amjad Ali.

Conversely, robotic prosthetic hands have become increasingly popular in recent years to improve the daily activities of persons with upper limb defects owing to accidents, diseases, congenital defects, etc. [11], [12], [13], [14], [15], [16]. Most robotic prosthetic hands have fewer finger joints or active joints than humans owing to link mechanisms. Furthermore, because it is difficult to operate the robot using a data glove or EMG balance due to upper limb deficiency in the case of amputees, limited degree of freedom (DOF) movements and grasping force control are performed using the EMG of the remaining muscles in the forearm and other parts of the body [17], [18]. Some methods are available to estimate the required hand posture based on the EMG patterns of the remaining muscles, postural changes in other parts of the body, and images of the object to be grasped for operating a robotic prosthetic hand with relatively high DOF [19], [20]. Although these methods have high accuracy of over 85% in achieving the target posture and significantly improve the user's daily activities, their versatility is limited considering they cannot achieve postures that have not been previously defined. Therefore, while robotic prosthetic hands operated by upper limb amputees can grasp objects such as cups and blocks well enough, they cannot perform sophisticated movements such as manipulating forks and chopsticks with the fingertips.

This study establishes a control method for upper limb amputees that enables the intended real-time manipulation of a robotic prosthetic hand with the same degree of freedom as a human finger. To develop a robotic hand for a person with a wrist deficiency, detailed information is required to indicate finger motion instead of using such devices as data gloves. Therefore, this study proposes a muscle activity estimator for defective muscles based on the activity of the remaining muscles. The proposed estimator applies the concept of ''muscle synergy'' and ''enslaving'' to evaluate the relationship between defective and non-defective muscles. Human motion is controlled by a large number of muscles, however, the burden on the brain is reduced by generating a signal that indicates the activity relationship of each muscle, called muscle synergy [21]. Methods for generating muscle synergies from EMG and vice versa have been proposed [22], [23]. Furthermore, muscle synergy has been studied in the field of robotics. There are methods to classify the posture of the robot hand based on the operator's muscle synergy or to realize precise manipulation using EMG through machine learning [24], [25]. In contrast, D'Avella et al. [26] analyzed muscle synergy patterns from arm and shoulder EMG in response to point-to-point movements of the paw of multiple subjects and concluded that there were similarities between subjects. Therefore, the activity of the deficient muscle can be estimated from the activity of the residual muscle of the prosthetic hand user using an estimator that has learned the synergy of the muscles that move the finger of healthy persons. Muscle activity is not only related to the anatomy but also to ''enslaving.'' Humans cannot perform an intended motion entirely independently and are accompanied by other unintended motions in parts of the body unrelated to the intended motion. This phenomenon has been investigated in anatomy and neurophysiology [27], [28]. During index finger abduction, the linkage of little finger abduction is prominent. Aoyama et al. [29] reported the neuronal activity to inhibit enslaving via the cortex by measuring the corticospinal excitability of the little finger abductor muscle during selective abduction and adduction of the index finger. Therefore, the motions of parts of the body not associated with the targeted muscles for estimation may also provide features to improve estimation accuracy.

The muscle activity of living organisms involves dynamics that change depending on the force of contraction of the muscle and the activity command from the brain [30]. These dynamics are unknown to the estimator. Kiguchi and Fukuda [31] improved the control accuracy by adding viscoelastic properties to each neuron in a multilayer neural network to compensate for the unmodeled and unknown dynamics in the environment and the robot. This indicates that the accuracy of muscle activity estimation can be improved by using an ANN with viscoelastic properties. Conversely, recurrent artificial neural networks (RNNs) are widely used to estimate continuous data such as EMG. In particular, a long-short-term memory neural network (LSTM) is often used to cope with the gradient loss problem in long-term estimation. Jabbari et al. [32] proposed a method to classify three levels of grasping force based on muscle contractions during grasping movements measured from the forearms of upper limb deficiencies. Simão et al. [33] proposed an ANN to recognize hand posture from forearm EMG patterns while comparing multiple RNNs, including LSTM. Moreover, significant research has been conducted controlling of robot manipulators in methods that generate linear control signals rather than posture recognition [34]. Accordingly, the LSTM with cells containing viscoelastic properties may improve the accuracy of muscle activity estimation. This study proposes a method for estimating muscle activity to compensate for the missing input signal when an upper limb amputee uses a myoelectric prosthetic hand. Instead of the conventional method of simple grasping motions and switching between several different postures, the proposed estimator enables continuous and detailed manipulation similar to that of a human hand. The LSTM-D, which is a fusion of an ANN with viscoelastic properties and an LSTM for learning time-series data, is proposed for the estimator and its performance is evaluated.

II. OVERVIEW OF MUSCLE ACTIVITY ESTIMATOR

The proposed muscle activity estimator learns muscle synergy by taking as input the activity of muscles anatomically or by enslaving related to the muscle to be estimated, the movement (joint angle) in which the target muscle is involved, and the grasping force. This study evaluates the performance of the estimator by assuming the case where the estimator is incorporated into the prosthetic finger robot system, as shown in Fig. 1. This finger robot mimics the tendons connected to the extensor, flexor digitorum profundus (FDP), flexor digitorum superficialis (FDS), and Volar/Dorsal interosseous muscle (Volar/ Dorsal IM) that control the movement of the index finger [10]. The posture of the finger changes according to the tension balance of the five tendons. The tension balance of the five tendons is proportional to the EMG balance of the corresponding muscles, and the EMG signals measured by the user can be processed by root mean square (RMS) and normalized by the maximum voluntary muscle contraction (%MVC). The processed signals are proportional to the tension of each tendon and are input as command values to the robot controller. The sampling frequency of EMG is 1000. The recorded EMG data are preprocessed via a band pass filter of 15-1,000Hz. The processing period of RMS is 200 samples. Because the interosseous muscle signals are

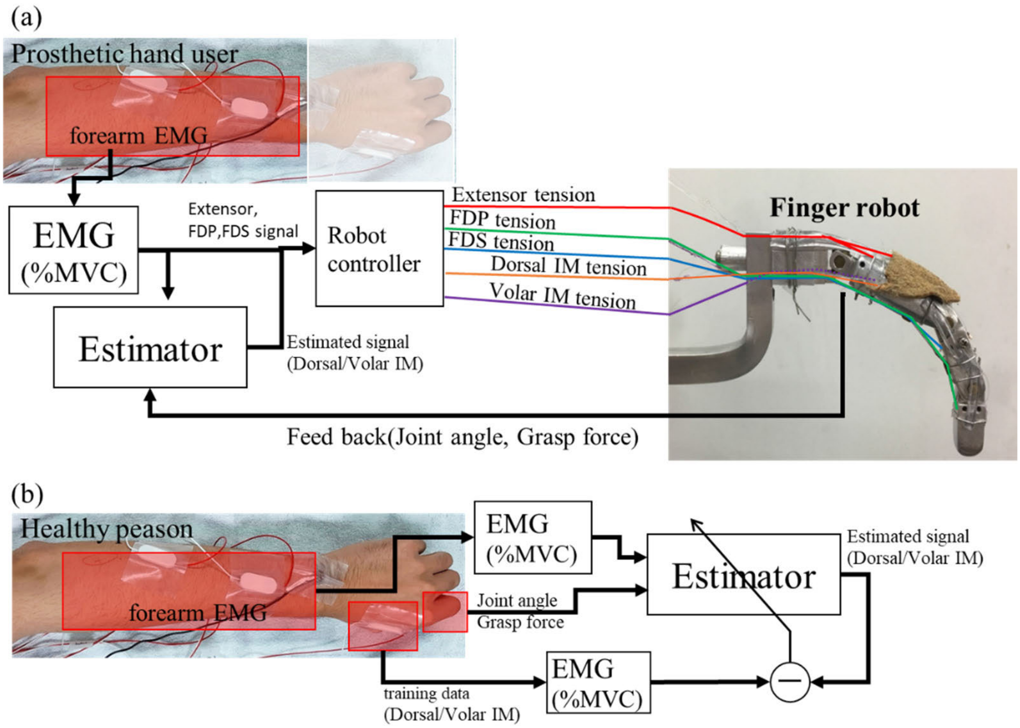

FIGURE 1. Prosthetic finger control system. (a) Signal flow to the estimator and the robot controller when a prosthetic hand user operates the finger robot and (b) training of the estimator using the forearm and hand EMG, finger joint angles, and grasping force of healthy subjects as inputs.

missing when the prosthetic finger robot is operated by a wrist amputee, the muscle activity of the Dorsal IM is estimated by the forearm muscle activity in this paper. The Dorsal IM contributes significantly to the abduction of the index finger. Furthermore, because the Dorsal IM is connected to the metacarpal and basal and metacarpal bones of the index finger and thumb, respectively, the activity of the Dorsal IM causes abduction and adduction of the index finger and thumb, respectively. To selectively operate the index finger, adduction of the thumb is inhibited by the abductor pollicis longus (APL) muscle in the forearm. Furthermore, abduction of the index finger causes muscle activity to abduct or inhibit abduction of the little finger by enslaving. Therefore, the muscle activity estimator learns the relationship between the extensor, FDP, FDS, APL, and the extensor digiti minimi (EDM) in the forearm and the Dorsal IM, which is the estimation target. All muscle activities are processed in the same way as the EMG balance signal. Additionally, the joint angles (4DOF) and grasping force feedback from the robot are included as inputs. The joint angles are normalized within $\pm 90°$, and the grasping force is normalized by the maximum value of the force sensing resistor (FSR). The input and output signals are shown in Table 1.

TABLE 1. Input signals for estimator.

	INPUT	Data format
Muscle activity	Extensor	EMG normalized by maximal voluntary muscle contraction 0 to 1
	FDP	
	FDS	
	APL	
	EDM	
Joint angle	MP (extension/flexion)	Normalized -90° to 90° degree → -1 to 1
	MP (abduction)	
	DIP	
	PIP	
Grasp force	Pinch	Normalized 0 to 1
	Grasp	
	Lateral Pinch	
	OUTPUT	
Muscle activity	Dorsal IM	0 to 1

III. DESIGN OF LSTM WITH INTEGRATED DAMPING NEURONS

Fig. 2 shows the cell structure of the LSTM with integrated damping neurons (LSTM-D), which is the muscle activity estimator. The basic structure is the same as the LSTM structure along with the forget gate proposed by Gers et al. [35]. In an artificial neural network, the output y of a neuron using

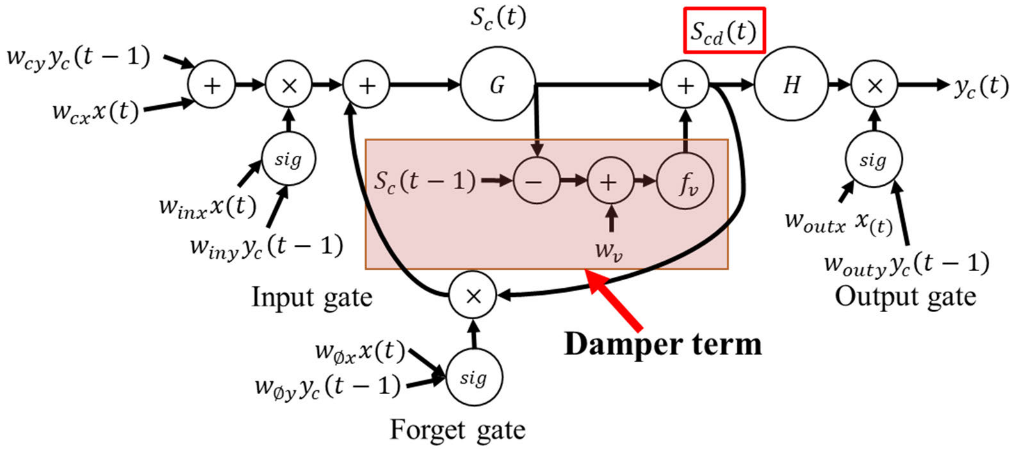

FIGURE 2. The LSTM-D cell structure. x: inputs to the cell, y_c: outputs of the cell, w_{**}: weights, G: sigmoid function taking values between −2 and 2, H: hyperbolic tangent, and f_v: sigmoid function taking values in the range 0 to 1.

the damping neuron concept is given as:

$$y = f_x\,(w_x x) + w_v f_v(\dot{f_x}\,(w_x x)) \tag{1}$$

where f_x is the activation function, w_x is the weight of input x, w_v is the weight of the damper terms, and f_v is the activation function of the damper terms [31]. In the proposed LSTM-D, S_{cd} with a damper term applied to the updated S_c is added to act on both long-term and short-term memory, given as:

$$S_{cd}\,(t) = S_c\,(t) + w_v f_v(\dot{S_c}\,(t)) \tag{2}$$

The evaluation function E in learning is represented by the error e from the target value and its derivative $\dot{e}$, given as:

$$E = \frac{1}{2}(K_x e + K_v \dot{e})^2 \tag{3}$$

According to the proposal of Kiguchi and Fukuda [31], K_x and K_v are coefficients given by the fuzzy rule. However, in this paper, $K_x = 0.9$ and $K_v = 0.1$.

IV. EXPERIMENT TO EVALUATE MUSCLE ACTIVITY ESTIMATOR

Assuming that the prosthetic finger user uses a pre-trained muscle activity estimator, the proposed estimator is trained using a healthy subject's finger motion data to estimate the other subjects' data in the evaluation experiment. Five healthy, right-handed subjects (age: 20–31 years, males) participated. The experimental protocol was approved by the research ethics committee of the Faculty of Engineering at Kyushu University (No. 2020-05). The subjects were asked to repeatedly perform eight index finger postures and three object grasps, as shown in Fig. 3, and the surface EMG of the Extensor, FDP, FDS, APL, EDM, and Dorsal IM were measured using an EMG amplifier (MEG-6116, Nihon Kohden), as shown in Fig. 4. The robot feedback (joint angle and grasp force) input to the estimator is the subject's index finger, which is measured simultaneously with the EMG. The joint angles were measured using potentiometers (Murata,

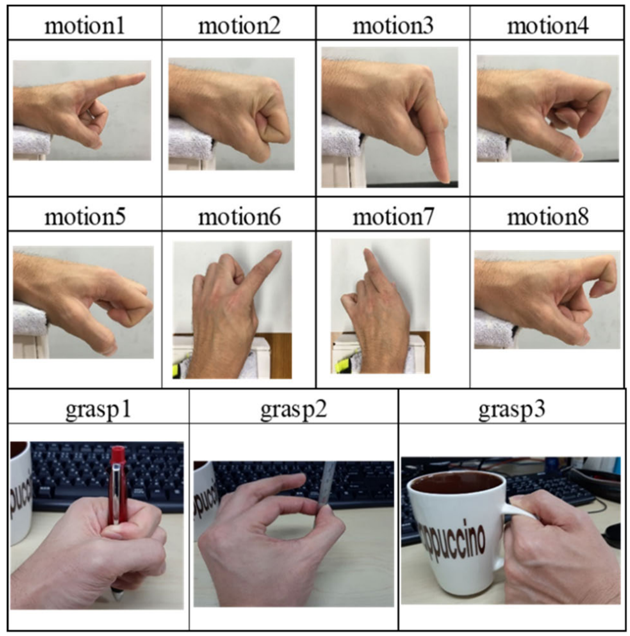

FIGURE 3. Finger movement patterns for estimator evaluation.

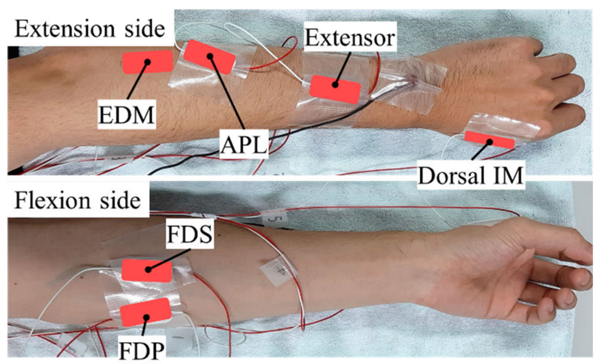

FIGURE 4. EMG electrodes location.

SV01A103AEA01B00). The grasping force was measured using force sensing resistors (FSRs), and one of the three

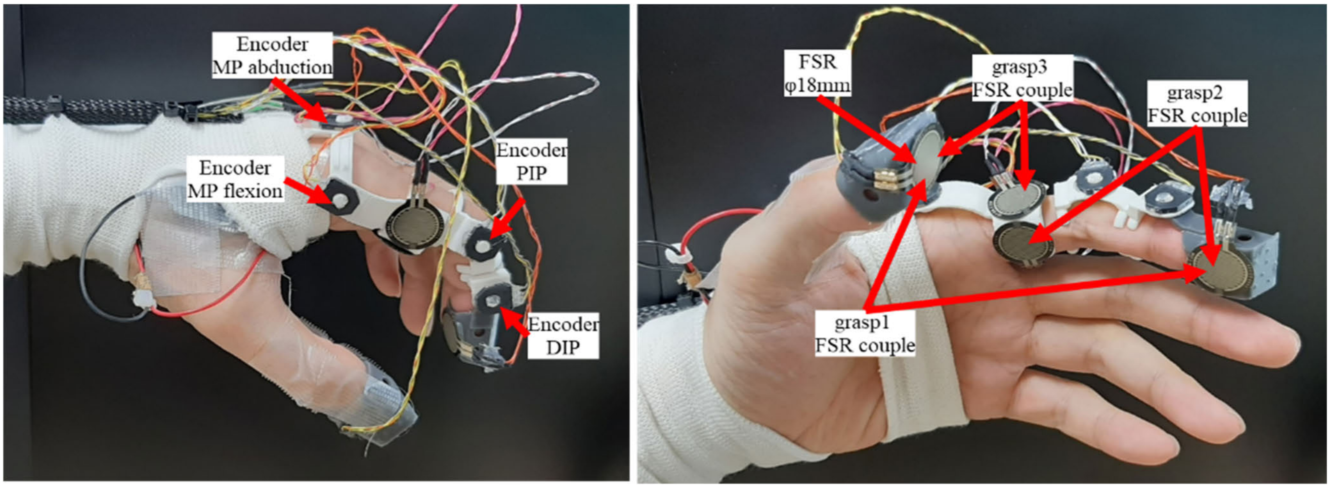

FIGURE 5. Sensors attached to the subject's finger: encoders to measure four joint angles and FSR couples to measure three different GRIPs.

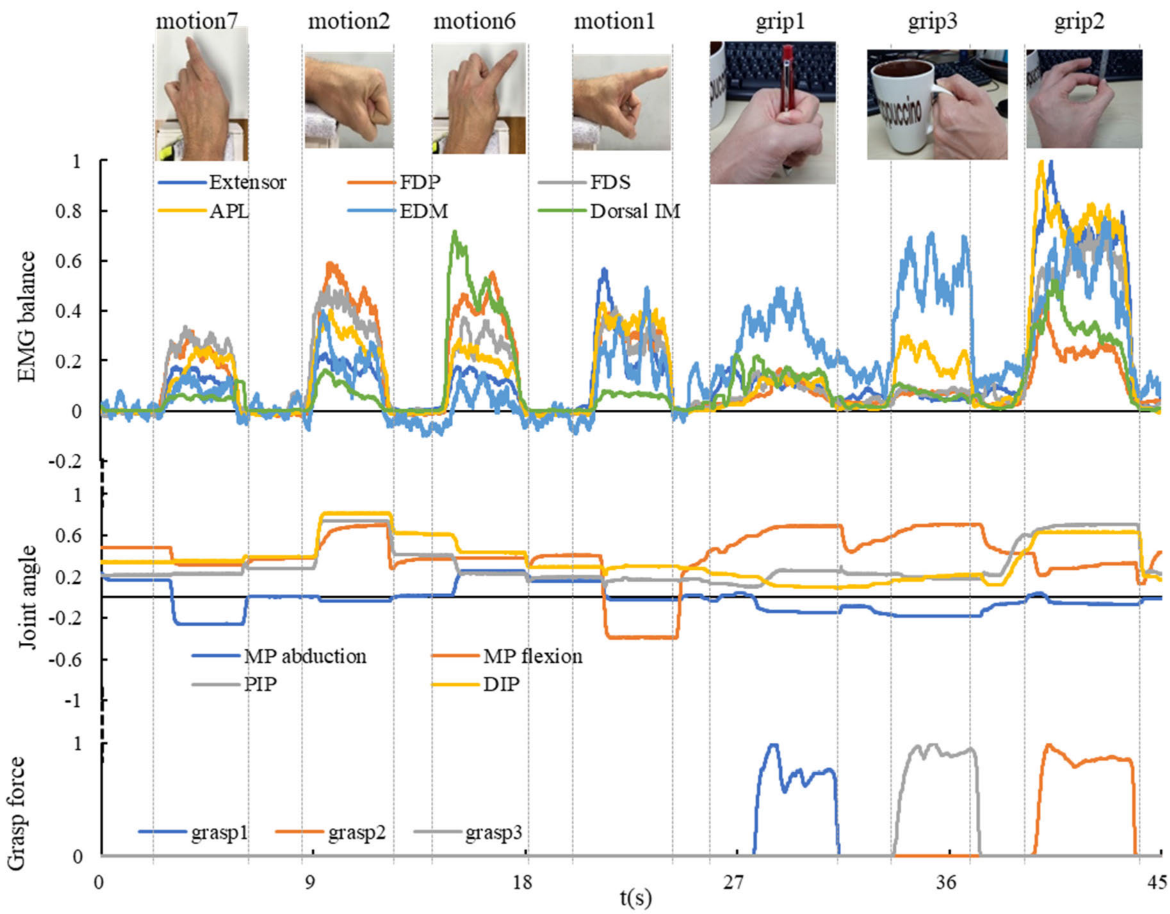

FIGURE 6. Data of subject 1: Each data is normalized. The grasping force is transformed so that three channels of signals are excited by the combination of four FSRs.

types of grasps was an opposing motion of the tip and the base of the index finger, while the other was the index finger and the thumb combined. Therefore, a total of four FSRs (Interlink Electronics, FSR402 short) were attached to the index finger and thumb to measure the grasp force. Fig. 5 shows the positions of the encoders for measuring joint angles and FSRs. In the measurement posture, the forearm is horizontal, and the palm is downward and placed on the table so

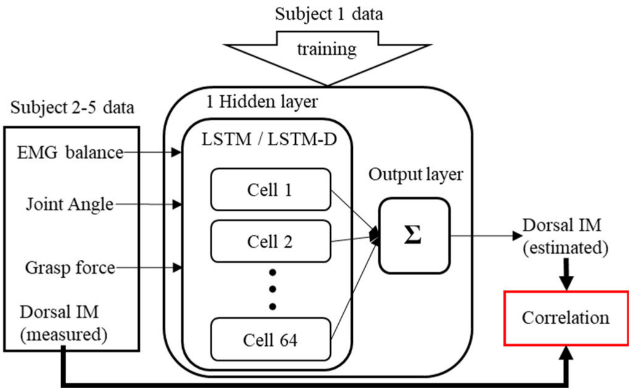

FIGURE 7. Configuration of the estimator evaluation experiment.

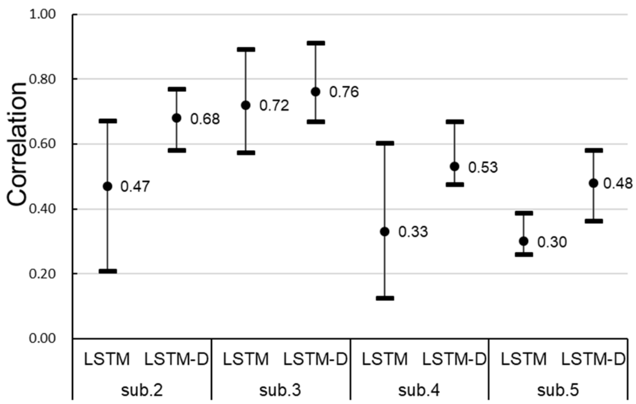

FIGURE 8. Correlation coefficients between the estimated results and measured data of each subject.

as not to interfere with the finger movements. The postures shown in Fig. 3 change in the following order: relax (3 s), change posture (1 s), hold posture (3 s), and return to relax (1 s). Each subject performed six sets of measurements, each set comprising data from eight different postures and three different grasping movements performed once in random order. The sampling frequency is 1,000 Hz. Each data set measures about 90,000 samples, which can vary depending on the speed of the subject's motions. Fig. 6 shows a part of the data of subject 1, which was used as training data, while the data of subjects 2 - 5 were used as test data for training and evaluation of the estimator. Fig.7 shows the configuration of the estimator. The hidden layer is one layer, which is either an LSTM-D with 64 cells or a normal LSTM. The output layer is a linear function. The training coefficient is set to 0.0001 and the number of training cycles is 1,400.

V. EXPERIMENTAL RESULT

Fig. 8 shows the correlation coefficients between each subject's estimated results and the measured data. The values are the mean values of the correlation coefficients for the six sets of test data for each subject, and the error bars indicate the maximum and minimum values. The correlation coefficients between the LSTM-D results and the measured values are higher than those of LSTM for the data of all subjects, which indicates that LSTM-D has a higher estimation accuracy than LSTM. Additionally, the variance is smaller in subjects 2, 3, and 4 considering the damper term absorbs the difference in muscle activity generated by the subject's repetitive movements. Fig. 9 shows the estimated results for one set of movements for each subject, whereas the LSTM results show large oscillations and the LSTM-D results suppress the

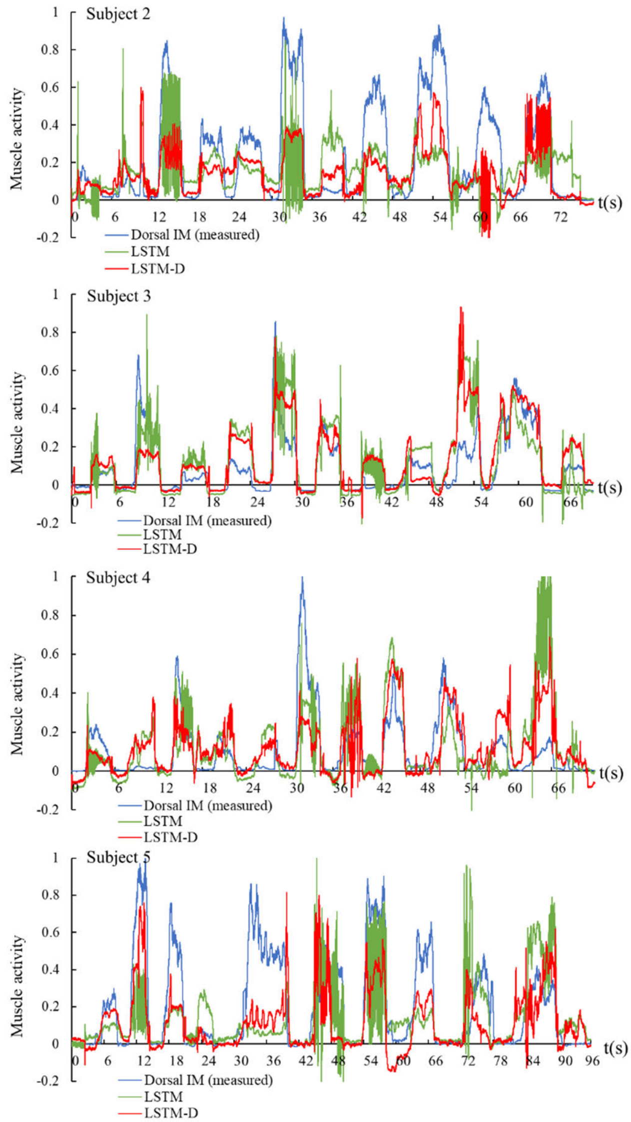

FIGURE 9. Estimated results for one set of test data for each subject.

TABLE 2. Root mean squared error.

subject No.	LSTM	LSTM-D
2	0.209	0.181
3	0.139	0.120
4	0.190	0.154
5	0.238	0.209

TABLE 3. Correlation coefficients for combinations of training and test data.

Trainin g data	Test data 1	2	3	4	5
1	-	0.47	0.72	0.33	0.30
2	0.47	-	0.65	0.53	0.43
3	0.58	0.40	-	0.43	0.14
4	0.42	0.56	0.69	-	0.26
5	0.35	0.54	0.38	0.62	-

vibrations. This is one of the reasons why the correlation coefficient of LSTM-D is higher than that of LSTM for the performance of the muscle activity estimator, considering it can estimate the subject's muscle tension or relaxation states in real-time. However, this experiment was evaluated with pre-prepared data. The mean squared error (RMSE) of the LSTM-D estimation results for each subject shown in Table 2 is better than that of the LSTM results for all subjects. Several applications use LSTM to estimate time series data, including biosignals, weather, energy, and traffic [36], [37], [38], [39], [40]. In each case, RMSE is approximately 0.1 when the range of estimated value is set between 0 to 1, which is similar to the performance of the model proposed in this study. However, the error is approximately 20%, whereas the range of muscle activity is between 0 to 1, which indicates that the accuracy of estimation still needs to be improved. Additionally, the estimated results when the data set of subjects used for training is changed is shown in Table 3 in correlation coefficients with the measured data. When subjects 1-4 are used for training, the test results for subject 3 are better, but the correlations for subject 5 are low. These results are the similarity among subjects of muscle synergy shown by D'Avella et al. [26], but with individual differences, therefore, more subjects will need to be evaluated in the future.

VI. CONCLUSION

This study proposed a method to estimate the amount of activity of the interosseous muscles of the missing hand of a wrist amputee using a humanoid robot prosthesis. An estimator takes as input the muscle activity of the prosthesis user's forearm, robot hand posture, and grasping force, and contains an LSTM that has been previously trained using data from a healthy subject. Furthermore, we propose LSTM-D, which combines LSTM with a damping neuron to estimate the states of muscle tension or relaxation and posture change in real-time with higher accuracy than conventional LSTM, allowing continuous control without definition; conversely, existing multi-fingered robotic prosthetic hands are controlled discontinuously by switching posture patterns. In the future, the performance of the estimator will be evaluated using data from upper limb amputees, and real-time estimation will be performed. Although this paper focuses on the estimation of the activity of interosseous muscles, it can also be used to estimate the activity of various deficient muscles. Furthermore, the estimation of muscle activity, which is a biological signal, can be applied to prosthetic hand operations as well as rehabilitation.

REFERENCES

[1] T. Mouri and H. Kawasaki, "A novel anthropomorphic robot hand and its master slave system," in *Humanoid Robots, Human-like Machines*. I-Tech Education and Publishing, Jun. 2007, doi: 10.5772/4796.

[2] M. Mishima, H. Kawasaki, T. Mouri, and T. Endo, "Haptic teleoperation of humanoid robot hand using three-dimensional force feedback," *IFAC Proc. Volumes*, vol. 42, no. 16, pp. 431–436, 2009, doi: 10.3182/20090909-4-JP-2010.00074.

[3] S. Tachi, K. Komoriya, K. Sawada, T. Nishiyama, T. Itoko, M. Kobayashi, and K. Inoue, "Telexistence cockpit for humanoid robot control," *Adv. Robot.*, vol. 17, no. 3, pp. 199–217, Jan. 2003, doi: 10.1163/156855303764018468.

[4] Y. Liu, Y.-Y. Tsai, B. Huang, and J. Guo, "Virtual reality based tactile sensing enhancements for bilateral teleoperation system with in-hand manipulation," *IEEE Robot. Autom. Lett.*, vol. 7, no. 3, pp. 6998–7005, Jul. 2022, doi: 10.1109/LRA.2022.3161711.

[5] Z. Xu and E. Todorov, "Design of a highly biomimetic anthropomorphic robotic hand towards artificial limb regeneration," in *Proc. IEEE Int. Conf. Robot. Autom. (ICRA)*, May 2016, pp. 3485–3492.

[6] D.-H. Lee, J.-H. Park, S.-W. Park, M.-H. Baeg, and J.-H. Bae, "KITECH-Hand: A highly dexterous and modularized robotic hand," *IEEE/ASME Trans. Mechatronics*, vol. 22, no. 2, pp. 876–887, Apr. 2017, doi: 10.1109/TMECH.2016.2634602.

[7] A. D. Deshpande, Z. Xu, M. J. V. Weghe, B. H. Brown, J. Ko, L. Y. Chang, D. D. Wilkinson, S. M. Bidic, and Y. Matsuoka, "Mechanisms of the anatomically correct testbed hand," *IEEE/ASME Trans. Mechatronics*, vol. 18, no. 1, pp. 238–250, Feb. 2013, doi: 10.1109/TMECH.2011.2166801.

[8] H. Zhou, Q. Zhang, M. Zhang, S. Shahnewaz, S. Wei, J. Ruan, X. Zhang, and L. Zhang, "Toward hand pattern recognition in assistive and rehabilitation robotics using EMG and kinematics," *Frontiers Neurorobotics*, vol. 15, May 2021, Art. no. 659876, doi: 10.3389/fnbot.2021.659876.

[9] M. Barsotti, S. Dupan, I. Vujaklija, S. Došen, A. Frisoli, and D. Farina, "Online finger control using high-density EMG and minimal training data for robotic applications," *IEEE Robot. Autom. Lett.*, vol. 4, no. 2, pp. 217–223, Apr. 2019, doi: 10.1109/LRA.2018.2885753.

[10] D. Tokunaga and K. Kiguchi, "Surface EMG based control for a humanoid finger robot," in *Proc. Syst. Integr. Division (SI), SICE*, Kagawa, Japan, 2019, p. 2D5-07.

[11] A. Fougner, Ø. Stavdahl, P. J. Kyberd, Y. G. Losier, and P. A. Parker, "Control of upper limb prostheses: Terminology and proportional myoelectric control—A review," *IEEE Trans. Neural Syst. Rehabil. Eng.*, vol. 20, no. 5, pp. 663–677, Sep. 2012, doi: 10.1109/TNSRE.2012.2196711.

[12] K. Ziegler-Graham, E. J. MacKenzie, P. L. Ephraim, T. G. Travison, and R. Brookmeyer, "Estimating the prevalence of limb loss in the United States: 2005 to 2050," *Arch. Phys. Med. Rehabil.*, vol. 89, no. 3, pp. 422–429, Mar. 2008, doi: 10.1016/j.apmr.2007.11.005.

[13] A. Esquenazi and R. H. Meier III, "Rehabilitation in limb deficiency. 4. Limb amputation," *Arch. Phys. Med. Rehabil.*, vol. 77, no. 3, pp. 18–28, 1996.

[14] D. R. Merrill, J. Lockhart, P. R. Troyk, R. F. Weir, and D. L. Hankin, "Development of an implantable myoelectric sensor for advanced prosthesis control," *Artif. Organs*, vol. 35, no. 3, pp. 249–252, Mar. 2011, doi: 10.1111/j.1525-1594.2011.01219.x.

[15] T. Chin, "Current status and views on the future of myoelectric prosthesis," *Jpn. J. Rehabil. Med.*, vol. 55, no. 5, pp. 394–399, 2018, doi: 10.2490/jjrmc.55.394.

[16] J. Kawamura et al., "The upper-limb amputees—A survey and trends in Kinki area of Japan," *Jpn. J. Rehabil. Med.*, vol. 36, no. 6, pp. 384–389, 1999.

[17] I. Vujaklija, D. Farina, and O. Aszmann, "New developments in prosthetic arm systems," *Orthopedic Res. Rev.*, vol. 8, pp. 31–39, Jul. 2016, doi: 10.2147/ORR.S71468.

[18] J. T. Belter, J. L. Segil, A. M. Dollar, and R. F. Weir, "Mechanical design and performance specifications of anthropomorphic prosthetic hands: A review," *J. Rehabil. Res. Develop.*, vol. 50, no. 5, pp. 599–618, 2013, doi: 10.1682/jrrd.2011.10.0188.

[19] Y. Fang, N. Hettiarachchi, D. Zhou, and H. Liu, "Multi-modal sensing techniques for interfacing hand prostheses: A review," *IEEE Sensors J.*, vol. 15, no. 11, pp. 6065–6076, Nov. 2015, doi: 10.1109/JSEN.2015.2450211.

[20] M. Khezri and M. Jahed, "Real-time intelligent pattern recognition algorithm for surface EMG signals," *Biomed. Eng. OnLine*, vol. 6, no. 1, p. 45, 2007, doi: 10.1186/1475-925X-6-45.
[21] N. Bernstein, *The Co-Ordination and Regulation of Movement*. Oxford, U.K.: Pergamon Press, 1967.
[22] A. d'Avella, P. Saltiel, and E. Bizzi, "Combinations of muscle synergies in the construction of a natural motor behavior," *Nature Neurosci.*, vol. 6, pp. 300–308, Mar. 2003, doi: 10.1038/nn1010.
[23] S. Hagio and M. Kouzaki, "Muscle synergies of human lower limb based on motor output," *Adv. Exerc. Sports Physiol.*, vol. 19, no. 1, pp. 1–6, 2013.
[24] M. Ison, I. Vujaklija, B. Whitsell, D. Farina, and P. Artemiadis, "Simultaneous myoelectric control of a robot arm using muscle synergy-inspired inputs from high-density electrode grids," in *Proc. IEEE Int. Conf. Robot. Autom. (ICRA)*, May 2015, pp. 6469–6474, doi: 10.1109/ICRA.2015.7140108.
[25] A. Furui, S. Eto, K. Nakagaki, K. Shimada, G. Nakamura, A. Masuda, T. Chin, and T. Tsuji, "A myoelectric prosthetic hand with muscle synergy–based motion determination and impedance model–based biomimetic control," *Sci. Robot.*, vol. 4, no. 31, Jun. 2019, doi: 10.1126/scirobotics.aaw6339.
[26] A. d'Avella, A. Portone, L. Fernandez, and F. Lacquaniti, "Control of fast-reaching movements by muscle synergy combinations," *J. Neurosci.*, vol. 26, no. 30, pp. 7791–7810, Jul. 2006, doi: 10.1523/jneurosci.0830-06.2006.
[27] K. T. Reilly and M. H. Schieber, "Incomplete functional subdivision of the human multitendoned finger muscle flexor digitorum profundus: An electromyographic study," *J. Neurophysiol.*, vol. 90, no. 4, pp. 2560–2570, Oct. 2003, doi: 10.1152/jn.00287.2003.
[28] V. M. Zatsiorsky, Z.-M. Li, and M. L. Latash, "Enslaving effects in multi-finger force production," *Exp. Brain Res.*, vol. 131, no. 2, pp. 187–195, Mar. 2000, doi: 10.1007/s002219900261.
[29] T. Aoyama, F. Kaneko, Y. Ohashi, and Y. Kohno, "Neural mechanism of selective finger movement independent of synergistic movement," *Exp. Brain Res.*, vol. 237, no. 12, pp. 3485–3492, Dec. 2019, doi: 10.1007/s00221-019-05693-x.
[30] H. Kusumoto, H. J. Park, M. Yoshida, and K. Akazawa, "Simultaneous modulation of force generation and mechanical property of muscle in voluntary contraction," *Soc. Biomech. Jpn.*, vol. 12, pp. 211–220, 1994, doi: 10.3951/biomechanisms.12.211.
[31] K. Kiguchi and T. Fukuda, "Neural network controllers for robot manipulators application of damping neurons," *Adv. Robot.*, vol. 12, no. 3, pp. 191–208, Jan. 1997, doi: 10.1163/156855398X00145.
[32] M. Jabbari, R. N. Khushaba, and K. Nazarpour, "EMG-based hand gesture classification with long short-term memory deep recurrent neural networks," in *Proc. 42nd Annu. Int. Conf. IEEE Eng. Med. Biol. Soc. (EMBC)*, Jul. 2020, pp. 3302–3305, doi: 10.1109/EMBC44109.2020.9175279.
[33] M. Simão, P. Neto, and O. Gibaru, "EMG-based online classification of gestures with recurrent neural networks," *Pattern Recognit. Lett.*, vol. 128, pp. 45–51, Dec. 2019, doi: 10.1016/j.patrec.2019.07.021.
[34] L. Jin, S. Li, J. Yu, and J. He, "Robot manipulator control using neural networks: A survey," *Neurocomputing*, vol. 285, pp. 23–34, Apr. 2018, doi: 10.1016/j.neucom.2018.01.002.
[35] F. A. Gers, J. Schmidhuber, and F. Cummins, "Learning to forget: Continual prediction with LSTM," *Neural Comput.*, vol. 12, no. 10, pp. 2451–2471, Oct. 2000, doi: 10.1162/089976600300015015.
[36] J. Q. Wang, Y. Du, and J. Wang, "LSTM based long-term energy consumption prediction with periodicity," *Energy*, vol. 197, Apr. 2020, Art. no. 117197, doi: 10.1016/j.energy.2020.117197.
[37] C. Chen, Q. Zhang, M. H. Kashani, C. Jun, S. M. Bateni, S. S. Band, S. S. Dash, and K.-W. Chau, "Forecast of rainfall distribution based on fixed sliding window long short-term memory," *Eng. Appl. Comput. Fluid Mech.*, vol. 16, no. 1, pp. 248–261, Dec. 2022, doi: 10.1080/19942060.2021.2009374.
[38] Z. Zhao, M. Zhai, G. Li, X. Gao, W. Song, X. Wang, H. Ren, Y. Cui, Y. Qiao, J. Ren, L. Chen, and L. Qiu, "Study on the prediction effect of a combined model of SARIMA and LSTM based on SSA for influenza in Shanxi province, China," *BMC Infectious Diseases*, vol. 23, no. 1, p. 71, Feb. 2023, doi: 10.1186/s12879-023-08025-1.
[39] X. Chen, H. Chen, Y. Yang, H. Wu, W. Zhang, J. Zhao, and Y. Xiong, "Traffic flow prediction by an ensemble framework with data denoising and deep learning model," *Phys. A, Stat. Mech. Appl.*, vol. 565, Mar. 2021, Art. no. 125574, doi: 10.1016/j.physa.2020.125574.
[40] T. Li, M. Hua, and X. Wu, "A hybrid CNN-LSTM model for forecasting particulate matter (PM2.5)," *IEEE Access*, vol. 8, pp. 26933–26940, 2020, doi: 10.1109/ACCESS.2020.2971348.

DAIGO TOKUNAGA (Student Member, IEEE) received the B.E. degree from the Kumamoto College, National Institute of Technology, Japan, in 2011, and the M.E. degree in instrument and meter engineering from Kyushu University, Fukuoka, Japan, in 2013, where he is currently pursuing the D.E. degree. He was with Toyota Motor Kyushu Inc., from 2013 to 2019.

SATOSHI NISHIKAWA (Member, IEEE) received the B.E., M.A.S., and Ph.D. degrees from the University of Tokyo, Tokyo, Japan, in 2010, 2012, and 2015, respectively. He was at the University of Tokyo as a Project Assistant Professor until September 2015 and as an Assistant Professor until March 2021. He is currently an Associate Professor with the Department of Mechanical Engineering, Faculty of Engineering, Kyushu University, Japan. His research interests include sports robots, musculoskeletal systems, and bio-inspired robots. He is a member of the IEEE Robotics and Automation Society, the Robotics Society of Japan (RSJ), the Japan Society of Mechanical Engineers (JSME), the Japanese Society of Biomechanics (JSB), and the Japanese Society for Regenerative Medicine and Rehabilitation (JSRMR). He was a recipient of the 31st RSJ Young Investigation Excellence Award in 2016.

KAZUO KIGUCHI (Senior Member, IEEE) received the B.E. degree from Niigata University, Niigata, Japan, in 1986, the M.A.Sc. degree from the University of Ottawa, Ottawa, ON, Canada, in 1993, and the D.E. degree from Nagoya University, Nagoya, Japan, in 1997.

He was with Mazda Motor Corporation, from 1986 to 1989, and MHI Aerospace Systems Corporation, from 1989 to 1991. From 1994 to 1999, he was with the Niigata College of Technology, Niigata. He was with the Graduate School of Science and Engineering, Saga University, Japan, from 1999 to 2012. He is currently a Professor at the Department of Mechanical Engineering, Faculty of Engineering, Kyushu University, Japan. His research interests include biorobotics, human-assist robots, rehabilitation robots, and the application of robotics in medicine. He is a Senior Member of the IEEE Robotics and Automation, Systems, Man, and Cybernetics, Computational Intelligence, and Engineering in Medicine and Biology Societies and a member of the Robotics Society of Japan, the Japan Society of Computer-Aided Surgery, the Society of Biomechanisms Japan, and the Japanese Society for Medical and Biological Engineering. He is a fellow of the Japan Society of Mechanical Engineers (JSME) and the Society of Instrument and Control Engineers (SICE). He received the JSME Funai Award, the JSME Medal for Outstanding Paper, the JSME Medal for Distinguished Engineers, and the Lifetime Achievement Award at WAC2014.